

# HIGH-EFFICIENCY JAMMING SIGNAL AGAINST UAV/DRONES

## TÍN HIỆU GÂY NHIỄU HIỆU QUẢ CAO CHỐNG LẠI UAV/MÁY BAY KHÔNG NGƯỜI LÁI

Pham Viet Anh<sup>1</sup>, Ha Ngoc Khoan<sup>1</sup>, Dang Trung Hieu<sup>2</sup>, Tran Van Nghia<sup>3\*</sup>

<sup>1</sup>108 Military Central Hospital ; <sup>2</sup>Electric Power University ; <sup>3</sup>Air Force – Air Defense Academy

Ngày nhận bài: 12/01/2022, Ngày chấp nhận đăng: 25/03/2022, Phản biện: TS. Trần Xuân Lượng

### **Abstract:**

In this paper, the authors introduce a new signal used to efficiently jam the remote control and video transmission channels of unmanned aerial vehicles/drones (UAV/Dr) **that using orthogonal frequency division multiplexing (OFDM)** to protect targets from their threats. The jamming efficiency of the proposed signal is demonstrated by Matlab simulations. Simulation results show that, in comparison with white noise, the proposed jamming signal brings a significant increase in the error performance for the remote control and video transmission channels.

**Keywords:** Orthogonal frequency division multiplexing (OFDM); UAV/Drone; Jamming

### **Tóm tắt:**

Trong bài báo này, các tác giả đề xuất một tín hiệu mới được sử dụng để gây nhiễu hiệu quả các kênh truyền video và điều khiển từ xa của các thiết bị bay không người lái/máy bay không người lái (UAV/Dr) **sử dụng kỹ thuật ghép kênh phân chia theo tần số trực giao (OFDM)** để bảo vệ mục tiêu khỏi các mối đe dọa của chúng. Hiệu quả gây nhiễu của tín hiệu đề xuất được chứng minh thông qua mô phỏng Matlab. Kết quả mô phỏng cho thấy, so với nhiễu trắng, tín hiệu gây nhiễu được đề xuất làm tăng đáng kể hiệu suất lỗi đối với các kênh điều khiển từ xa và các kênh truyền video.

**Từ khóa:** Ghép kênh theo tần số trực giao (OFDM); UAV/Drone

## **1. INTRODUCTION**

Unmanned aerial vehicles (UAV) and drones are widely used in civilian, commercial, as well as military applications [1-3]. Remote control radio links utilize Gaussian frequency-shift keying signal (GFSK) with frequency-hopping spread spectrum (FHSS) and direct sequence spread spectrum (DSSS) that allow drones to operate in a high interference environment [4]. However, UAV/Drones are limited by line of sight (LOS) operation (see Fig. 1). The majority of illegal applications (for example, military purposes) require

UAVs to operate over distances of several hundred kilometers under conditions of NLOS (non-line of sight) and fast-moving environments.

Thanks to achievements of LOS & NLOS operation, strong anti-interference, and strong anti-multipath fading, the OFDM (orthogonal frequency division multiplexing) has been commonly adopted in various standards, such as digital video broadcasting (DVB) standard [5], WiFi [6], 4G/LTE [7], 5G, etc. OFDM technology, such as LTE, WiFi, and video transmission, eliminated the line of sight control limitations [8-11]

and was selected to design new generation multi-UAVremote controllers [11] (see Fig. 1).



**Fig. 1. General control modes.**

Nowadays, an airborne video link transmitter deployed in a variety of UAVs has become a very important device in their guidance and control system. In addition, video signal also supports UAV/drones to accomplish their missions, such as, in military applications, performing reconnaissance, controlling weapons to shoot down targets, dropping bombs, etc.

To mitigate threats from illegal purposes, it is necessary to deploy anti-drone systems in sensitive areas, such as airports, military units, and country borders. FHSS and/or DSSS-based remote controls can be more resilient to interferences, but will be more easily distinguished from other types of communications in the spectrum. Detection systems recognize signal characteristics and choose an adequate jamming method. Jammers generate a high-power signal transmitted over the same carrier frequency and the operation bandwidth of the detected drone to neutralize the radio control link [12-14].

For new generation UAV/drones, white noise may be chosen as a jamming signal against an OFDM-based video link

[15, 16]. This noise is able to interfere with all spectral components of the target signal. The principle consists in the formation of a more powerful noise, along the occupied band, to deteriorate the performance of the drone receiver by increasing the bit error rate (BER). However, it is noted that remote control systems are the main object of the existing anti-drone systems, while video processing systems are not disabled. In addition, jammers found in the literature focus on unarmed UAV/drones, which raises concerns among defense and security authorities.

The paper introduces a new jamming signal that is obtained by quadrature amplitude modulation (QAM) schemes and the OFDM technique, the targeted system of which is new generation UAV/drones based on the OFDM technique. The jamming signal not only blocks remote control communication but also interferes with the video channel for armed UAV/drones. The proposed jammer is a simple OFDM transmitter, whose input is a pseudorandom binary sequence. The OFDM signal of the jammer is clipped at a predetermined

threshold by using the clipping-and-filtering (CAF) method [17]. The clipping noise is filtered to eliminate out-of-band (OOB) radiation. To jam the OFDM signals of remote control and video channels, the jammer does not insert a cyclic prefix. This does not cause OOB radiation, and thus not interfering with other radio systems. Furthermore, the jamming signal has a reduced peak-to-average-power ratio (PAPR), which enhances the power amplifier efficiency. Matlab simulations show that jamming can be effective with low energy requirements with the same bit error probability. A high jamming efficiency is achieved because there is a high correlation between the jamming signal and the jammed target signal.

## 2. THE PROPOSED JAMMING MODEL AND PROBLEM FORMULATION

In OFDM systems, such as video transceivers for UAV/drones, a symbol has  $N$  QAM cells,  $\mathbf{X}=[X(0), X(1), \dots, X(N-1)]$  where  $N$  is a power of two, among them,  $N_{act}$  active subcarriers with index set  $\mathcal{R}_{ib}$  are located in the middle. They are called in-band (IB) subcarriers. The rest subcarriers are null and called inactive ones. In practice, the OFDM signal samples are obtained by  $L$  times oversampling ( $L \geq 1$ ) using zero-padding, i.e., the input of IDFT block is an vector of  $LN$  elements as  $\mathbf{S} = [S(0), S(1), \dots, S(LN-1)] = [X(0), \dots, X(N/2-1), 0, \dots, 0, X(N/2), \dots, X(N-1)]$ . The index set of the inactive subcarriers and zero-padding locations is denoted as  $\mathcal{R}_{oob}$ . Therefore, the oversampled OFDM signal samples can be expressed as:

$$s(n) = \frac{1}{\sqrt{N_{act}}} \sum_{k=0}^{LN-1} S(k) e^{j2\pi kn/LN}, 0 \leq n \leq LN-1 \quad (1)$$

where  $S(k)$  represents the data symbol carried by the  $k$ -th subcarrier.

When the additive white Gaussian noise is chosen as a jamming signal, it is possible to interfere with all subcarriers of the target OFDM signal. The white noise is commonly used to simulate background noise. Accordingly, the required noise power increases beyond a certain threshold so that there is a strong spreading and mixing of the spots in the constellation, making it difficult for the receiver to decode the signal appropriately (see Fig. 2b).

To achieve a high correlation, the authors propose a simple OFDM transmitter for the jammer. First, this jammer generates the pseudo-random binary sequence (PRBS) used as the input of the OFDM transmitter. Then, the PRBS is modulated using QAM constellations. Finally, the OFDM signal of the proposed jammer is obtained via an IDFT. The PRBS can be produced using linear-feedback shift registers [18] with one of the generator polynomials:

$$\begin{aligned} & x^{31} + x^{28} + 1 \\ & x^{23} + x^{18} + 1 \\ & x^{20} + x^3 + 1 \\ & x^{15} + x^{14} + 1 \end{aligned} \quad (2)$$

As seen in Fig. 2c, if the useful data (the video stream for the UAV video channel) and the PRBS bits are mapped into two distinct constellation points by the same subcarrier, the jamming signal will drive the received constellation point

outside of the required boundary. This is real because the pseudorandom binary sequence is different from the useful data.

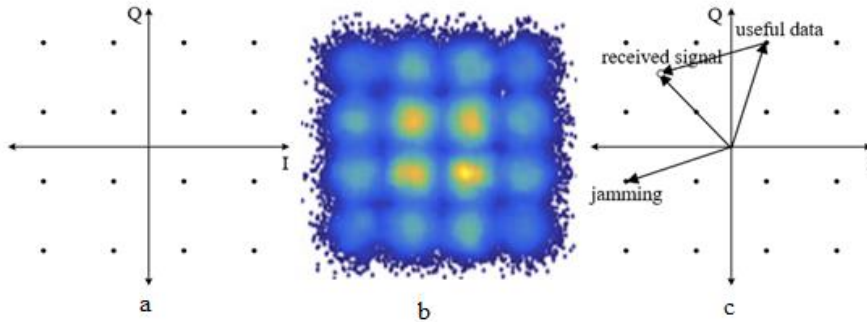


**Fig. 2. Jamming principles: (a) original 16-QAM constellation; (b) QAM signal plus white noise; (c) QAM signal plus the proposed jamming signal.**

It can be seen from equation (1), the signal  $s(n)$  is produced by adding the  $LN$  orthogonal subcarriers. Therefore, the instantaneous power of individual samples may be increased in comparison with the average signal power. The PAPR of  $s(n)$  is defined as the ratio of the maximum power to the average power:

$$\text{PAPR}\{s\} = \frac{\max_n |s(n)|^2}{E\{|s(n)|^2\}} \quad (3)$$

where  $E\{|s(n)|^2\}$  is the average power.

As a result, an extensive active range of power amplifiers (PA) is required in the transmitter, leading to a rise in cost and poor power efficiency. This problem

becomes urgent for portable wireless devices (including OFDM transmitter-based jammers) due to their limited battery power [17, 19]. In general, even linear PAs contain non-idealities that might reduce the effectiveness of the systems. A high-amplitude OFDM signal causes the PA to operate in the saturation area. This problem results in OOB emission, which affects the signals in neighboring bands and will draw more power from the transmitter. Moreover, high PAPR also demands the digital-to-analog converter (DAC) with high precision and dynamic range to decrease the quantization noise, which might be very expensive.

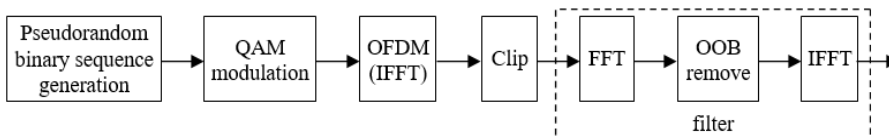


**Fig. 3. Proposed jammer block diagram.**

When deployed in the real world, PAPR reduction is one of the necessary solutions for OFDM technology since high PAPR presents a range of conflicting

requirements for system design decisions. The best solution is to reduce the PAPR before the OFDM signal is transmitted into the PA and DAC. Several efficient

PAPR reduction approaches, such as clipping and filtering (CAF), tone reservation, coding, active constellation extension, partial transmit sequence, selected mapping, and interleaving, have been analyzed in [17, 19]. Among PAPR reduction techniques, the CAF methods appear to be the simplest [19, Tab. 1]. Therefore, the CAF method in [17, subsection 3.2] is proposed for PAPR reduction of OFDM signal in the jammer. The block diagram of the proposed jammer is shown in Fig. 3.

The main idea of the CAF method is to clip the amplitude of the OFDM signal beyond a predefined threshold to reduce PAPR and then use a filter to eliminate OOB radiation. A clipping operation constrains the envelope of the time domain signal within the specified bounds while maintaining the signal phase. The clipped OFDM signal can be represented as follows:

$$\bar{s}(n) = \begin{cases} s(n), & |s(n)| \leq A \\ Ae^{j\theta(n)}, & |s(n)| > A \end{cases} \quad (4)$$

where  $A$  is the desired clipping threshold, and  $s(n) = |s(n)|e^{jq(n)}$  with  $\theta(n)$  is the phase of  $s(n)$ .

It can be seen from equation (4) that the clipped OFDM signal can be viewed as adding a noise source to the original OFDM signal. This additive signal is called clipping noise that represented as:

$$f(n) = \bar{s}(n) - s(n) \quad (5)$$

thus clipped OFDM signal in the time and frequency domains can be rewritten as:

$$\bar{s}(n) = f(n) + s(n) \quad (6)$$

The clipping noise is the difference between the samples of the original OFDM signal and its clipped version. From equations (4) and (5) we see that the clipping noise is a series of pulses that are non-zero at times when the OFDM signal exceeds the threshold  $A$ . Therefore, the frequency spectrum of clipping noise pulses is distributed over the whole frequency domain. It introduces OOB radiation (adjacent channel interference) into the communication systems. In order to satisfy the spectral constraint, a filter is required to eliminate the OOB emission. The frequency and impulse responses of the filter are given [17]:

$$H(k) = \begin{cases} 1, & k \in \mathfrak{R}_{ib} \\ 0, & \text{otherwise} \end{cases} \quad (7)$$

$$\begin{aligned} h(n) &= \frac{1}{\sqrt{N_{act}}} \sum_{k \in \mathfrak{R}_{ib}} e^{j2\pi kn/LN} \\ &= IDFT(\mathbf{H}) \end{aligned} \quad (8)$$

The proposed filter is based on a rectangular window. We could consider this filter as an  $LN$ -order finite impulse response (FIR) which performs a weighted sum (also known as discrete convolution) on a window of  $LN$  input data samples. The filter input is the clipped OFDM signal (4), (6). Thus the output of an  $LN$ -weight FIR filter is given by:

$$y(n) = \sum_{i=0}^{LN-1} h(n)\bar{s}(n-i) = \bar{s}(n) * h(n) \quad (9)$$

where  $*$  is the discrete convolution operation.

The output of the FIR filter can be expressed in the frequency domain by a DFT operation from (9) as:

$$Y(k) = \bar{S}(k)H(k) \quad (10)$$

From (7) we can see that the frequency response of the filter is defined by  $N_{act}$  elements of ones at the positions corresponding to the active subcarrier indices  $\mathcal{R}_{ib}$ . Likewise, the original OFDM signal in the frequency domain,  $\mathbf{S} = [S(0), S(1), \dots, S(LN-1)]$ , has  $N_{act}$  active subcarriers in the index set  $\mathcal{R}_{ib}$  while the rest subcarriers are null. Therefore, its output can be obtained as follows:

$$Y(k) = \bar{S}(k)H(k) = \begin{cases} \bar{S}(k), & k \in \mathcal{R}_{ib} \\ 0, & \text{otherwise} \end{cases} \quad (11)$$

$$y(n) = \text{IDFT}(\mathbf{Y}) \quad (12)$$

According to (11), the discrete frequency components of the filter input ( $\bar{s}(n)$ ) on the active (IB) subcarriers are passed on unchanged while the others (OOB components) are reset to zero. The filter consists of an FFT/IFFT pair. The clipped signal,  $\bar{s}(n)$ , is transformed to the frequency-domain via FFT operation to obtain  $\bar{S}(k)$ . The frequency domain filter passes without changing the IB discrete frequency components and resets the OOB components to zero. IB components are then applied to the input of the second IFFT to form the transmit signal.

The PAPR reduction capability is evaluated by using the Complementary Cumulative Distribution Function (CCDF). CCDF is defined by the probability that the PAPR of the OFDM

signal exceeds a given threshold  $\eta$  as follows:

$$\text{CCDF} = \Pr[\text{PAPR}\{\mathbf{s}\} > \eta] \quad (13)$$

BER vs signal-to-interference ratio (SIR) at the receiver side (UAV video signal receiver) is a performance measure of jamming methods, where the BER is the number of bit errors divided by the total number of transferred bits during a studied time interval, often expressed as a percentage, and SIR is measured from the receiver,

$$\text{SIR} = \frac{P_s}{P_I} \quad (14)$$

where  $P_s$  is the video signal power,  $P_I$  is the jamming signal power.

### 3. SIMULATION RESULTS

In this section, the authors evaluate PAPR reduction capability using the CCDF function and the performance of the proposed jamming method in terms of BER vs SIR. The jammed targets are the UAV remote control and video signal receivers based on the OFDM technique. In the simulations, we use the parameters of OFDM video transceivers of the Kimpok Company [11] in the 8K carrier mode and the 16-QAM constellation. The different modulation types, such as QPSK and 64-QAM modulation symbols are also presented in comparisons.

The PAPR reduction capability is measured by computing the symbol-wise CCDF. To approximate the continuous-time peak of the OFDM video signal, the oversampling rate factor is set to  $L = 4$ . It is well known that the CAF method eliminates the OOB radiation, but it results

in peak regrowth [17, 19, 20]. The regrowth peak power depends on the clipping threshold  $A$ . The simulations are carefully taken to search for the optimal target clipping level. Fig. 4 shows the achieved PAPR levels of the CAF method for different desired PAPR levels. The minimum achievable PAPR of 6.9 dB is obtained with an optimal clipping ratio of 6.5 dB.

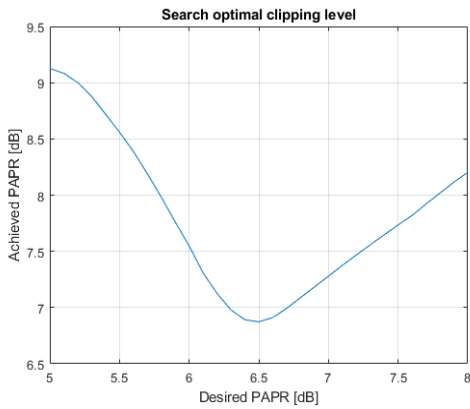


Fig. 4. The achievable PAPR of the proposed method with different target clipping ratios.

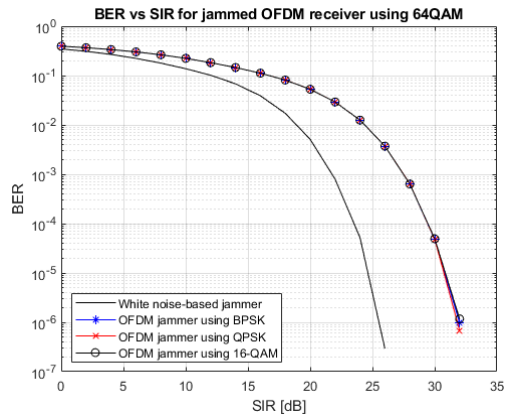
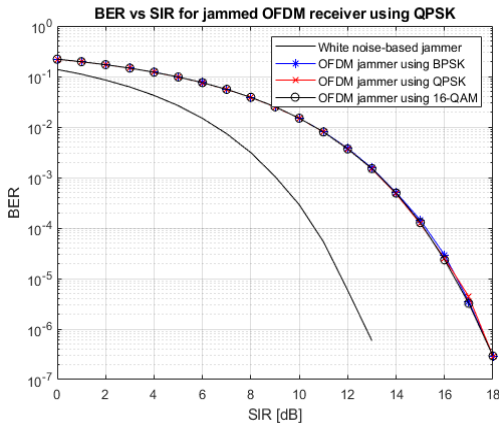


Fig. 5. Simulation results in the case of the OFDM signal-based jamming

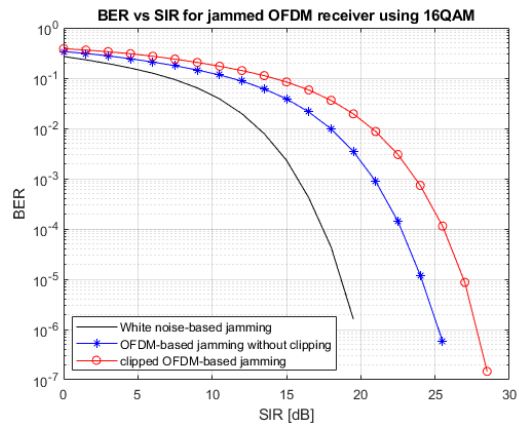


Fig. 6. Simulation results in the case of the clipped OFDM signal-based jamming.

To demonstrate the effect of the jamming method on the different modulation types, QPSK, 16-QAM, and 64-QAM modulation symbols are used as the input of the jammed systems, while BPSK, QPSK, and 16-QAM constellations are applied in the jammer. Simulation results shown in Fig. 5 and 6 are in the case of ignoring the channel model effect. White noise-based jamming is also presented in comparisons.

It can be seen from Fig. 5 and Fig. 6 that a higher-order constellation is more susceptible to jamming. The clipped OFDM signal-based jammer requires the

lowest power in experiments with a cost of increased complexity (see Fig. 3). This is because the clipping noise increases received constellation distortion. The red curve in Fig. 6 indicates the OFDM signal using BPSK clipped on a PAPR threshold of 6 dB. From the specific experiments in Fig. 4 we can see that if the jammed OFDM receiver has to endure a BER of 10%, it requires jamming signal power of 7 dB, 11 dB, and 14 dB at the receiver for white noise generator, OFDM signal-based jammer without clipping and clipped OFDM signal-based jammer, respectively.

#### 4. CONCLUSION

In this study, the authors have proposed a new signal used to efficiently jam the OFDM receivers of UAV/drones. The proposed jammer is based on a simple OFDM transmitter, whose input is a pseudorandom binary sequence. The clipping-and-filtering method is included to reduce the peak-to-average-power ratio of the jamming signal and increase the jamming capability. Simulation results from Matlab show that the proposed jammer achieves a low energy requirement with the same bit error probability as the white noise-based jammer does. Jamming capability is almost the same for any QAM modulation type. The clipped OFDM signal-based jammer requires the lowest power.

#### REFERENCES

- [1]. K. Wackwitz, L. Schroth and H. Bödecker, "Drone Application Report 2021," Drone Industry Insights, (2021).
- [2]. Constant and Sophia, "NHS launches UK's first COVID test drone delivery service in Scotland," Skyports, 2021.
- [3]. A. Rogers and J. Hill, "Unmanned: Drone Warfare and Global Security," Between the Lines. ISBN 9781771131544, (2014).
- [4]. M. Rabiai, M. R. Senouci, A. Senouci, K. Busawon and L. Dala, "A hardware solution to overcome the bandwidth limitation of drone jamming platforms," 2020 12th International Symposium on Communication Systems, Networks and Digital Signal Processing (CSNDSP), 2020, pp. 1-4, doi: 10.1109/CSNDSP49049.2020.9249517.
- [5]. EN302755, "Digital video broadcasting (DVB); frame structure channel coding and modulation for a second generation digital terrestrial television broadcasting system," European Telecommunications Standards, 2015.
- [6]. E. Khorov, A. Kiryanov, A. Lyakhov and G. Bianchi, "A Tutorial on IEEE 802.11ax High Efficiency WLANs," in IEEE Communications Surveys & Tutorials, vol. 21, no. 1, pp. 197-216, Firstquarter 2019, doi: 10.1109/COMST.2018.2871099.
- [7]. 3GPP TS 36.211, "Evolved Universal Terrestrial Radio Access (E-UTRA); Physical channels and modulation," 3rd Generation Partnership Project, 2017.

- [8]. R. Curpen, T. Bălan, I. A. Micloş and I. Comănici, "Assessment of Signal Jamming Efficiency Against LTE UAVs," 2018 International Conference on Communications (COMM), 2018, pp. 367-370, doi: 10.1109/ICComm.2018.8484746.
- [9]. F. Minucci, E. Vinogradov, H. Sallouha and S. Pollin, "UAV Location Broadcasting with Wi-Fi SSID," 2019 Wireless Days (WD), 2019, pp. 1-8, doi: 10.1109/WD.2019.8734208.
- [10]. H. Li et al., "Cellular Based Small Unmanned Aircraft Systems MIMO Communications," 2019 Integrated Communications, Navigation and Surveillance Conference (ICNS), 2019, pp. 1-6, doi: 10.1109/ICNSURV.2019.8735229.
- [11]. Kimpok company, "High Power COFDM Video Transmitter 50km NLOS Long Range Wireless Transmitter and Receiver," <http://www.kimpok.com>, Retrieved May 2021.
- [12]. B. Taha and A. Shoufan, "Machine Learning-Based Drone Detection and Classification: State-of-the-Art in Research," in IEEE Access, vol. 7, pp. 138669-138682, 2019, doi: 10.1109/ACCESS.2019.2942944.
- [13]. J. Marin, M. Heino, J. Saikanmäki, M. Mäenpää, A. -P. Saarinen and T. Riihonen, "Perfecting Jamming Signals Against RC Systems: An Experimental Case Study on FHSS with GFSK," 2020 IEEE 31st Annual International Symposium on Personal, Indoor and Mobile Radio Communications, 2020, pp. 1-5, doi: 10.1109/PIMRC48278.2020.9217129.
- [14]. X. Shi, C. Yang, W. Xie, C. Liang, Z. Shi and J. Chen, "Anti-Drone System with Multiple Surveillance Technologies: Architecture, Implementation, and Challenges," in IEEE Communications Magazine, vol. 56, no. 4, pp. 68-74, April 2018.
- [15]. P. Čisar, R. Pinter, S. M. Čisar and M. Gligorijević, "Principles of Anti-Drone Defense," IEEE International Conference on Cognitive Infocommunications (CogInfoCom), 2020, pp. 19-26, doi: 10.1109/CogInfoCom50765.2020.9237841.
- [16]. S. Park, H. T. Kim, S. Lee, H. Joo and H. Kim, "Survey on Anti-Drone Systems: Components, Designs, and Challenges," IEEE Access, vol. 9, pp. 42635-42659, 2021, doi: 10.1109/ACCESS.2021.3065926.
- [17]. V.-N. Tran, "Low complexity reconfigurable complex filters for PAPR reduction of OFDM signals: analysis, design and FPGA implementation," IET Communications, 2018, vol. 12, Iss. 13, pp. 1531-1539, DOI: 10.1049/iet-com.2017.1098.
- [18]. J. Hu, Z. Zhang and Q. Pan, "A 15-Gb/s 0.0037-mm<sup>2</sup> 0.019-pJ/Bit Full-Rate Programmable Multi-Pattern Pseudo-Random Binary Sequence Generator," IEEE Transactions on Circuits and Systems II: Express Briefs, vol. 67, no. 9, pp. 1499-1503, Sept. 2020, doi: 10.1109/TCSII.2020.3008567.
- [19]. Y. Rahmatallah and S. Mohan, "Peak-To-Average Power Ratio Reduction in OFDM Systems: A Survey And Taxonomy," IEEE Communications Surveys Tutorials, vol. 15, no. 4, March 2013, pp. 1567-1592.
- [20]. S. Wang, M. Roger and C. Lelandais-Perrault, "Impacts of Crest Factor Reduction and Digital Predistortion on Linearity and Power Efficiency of Power Amplifiers," IEEE

Transactions on Circuits and Systems II: Express Briefs, vol. 66, no. 3, pp. 407-411, March 2019.